

Analysis of the effect of a white coextruded layer on the development of solar radiation-induced wrinkles in Polyethylene geomembranes

David Beaumier, Patricia I. Dolez & Eric Blond
SAGEOS/CTT Group, Canada

Doyin Adesokan
Solmax International, Canada

ABSTRACT: Polyethylene geomembranes have historically been manufactured using carbon black in their formulation to improve their resistance to ageing due to UV radiation. The black color, on the other hand, absorbs most of the solar energy reaching the surface. The temperature rise induced in the geomembrane is the source of numerous problems in the field, including the formation of wrinkles, thermo-oxidative degradation of the polymer, and desiccation of the soil located underneath. In order to minimize this issue, a fine white layer can be added on the exposed surface of the geomembrane using titanium dioxide pigments for instance in the formulation. It is intended to reflect the solar radiation and therefore, reduce the geomembrane temperature.

This paper presents the results of a study aimed at quantifying the difference in heat generation under solar irradiation associated with the presence of the white surface layer. The temperature of black only and white/black geomembrane specimens was measured while they were exposed to various laboratory-controlled solar irradiances using a Xenon-arc chamber modified for the purpose of this project. The coefficient of thermal expansion of these geomembranes was also determined by thermomechanical analysis. Temperature was found to be significantly lower in the white-surfaced geomembranes, compared to the black ones, with differences in the range of 25°C. The thermal expansion was reduced by up to 55-60%.

These results were combined with climatic data for Toronto, Canada, to quantify the effect of the white layer on the geomembrane thermal expansion. The calculated thermal expansion is used to estimate the effect of the white layer on the generation of wrinkles caused by solar radiation, and conditions for installation and service operations of exposed geomembranes.

Keywords: Geomembrane; effect of surface color; white surface; solar radiation-induced heating; wrinkles; thermal expansion; weatherability

1 INTRODUCTION

Polyethylene geomembranes have historically been manufactured using carbon black in their formulation to improve their resistance to ageing due to ultraviolet (UV) radiation. Indeed, polyethylene is sensitive to UV, due to the unavoidable presence of chromophoric impurities that lead to parasitic photo-initiation above the 180nm absorption cutoff value of the polymer itself (Struick 1985). Degradation then proceeds by free radical-mediated oxidation. The reaction is thermally activated.

Polyethylene becomes brittle and its mechanical performance rapidly decreases as a result of UV aging. For instance, the loss in tensile strength and elongation may be up to 50% after half a year to one year of exposure to outdoor conditions (Struick 1985). This is an issue for polyethylene-based products, such as geomembranes that may be left exposed to sunlight for extended periods.

Carbon black has traditionally been added to the polyethylene geomembrane formulation to improve their resistance to UV aging (Scheirs 2009). The amount of carbon black used is generally 2-3%. Carbon black acts by absorbing the damaging UV radiation as well as scavenging the free radicals formed by the

photo-oxidation reaction. When carbon black is combined with the right choice of antioxidant package, the service-life of polyethylene geomembranes in exposed conditions can be considerably improved. For instance, a high density polyethylene (HDPE) geomembrane left exposed in a warm environment for 16 years exhibited no failure, even though its residual resistance to stress cracking had reached an alarming low level (Rowe & Ewais 2015).

However, adding carbon black to geomembrane formulations also leads to undesirable consequences. Due to their color, black geomembranes absorb most of the solar energy reaching their surface (Pelte et al. 1994). This generates an increase in their temperature compared to ambient conditions. For instance, a black HDPE geomembrane exposed on a site near Philadelphia, PA, reached a maximum temperature of 70°C in summer time whereas the ambient temperature was only 30°C (Koerner and Koerner, 1995). Because of the large coefficient of linear thermal expansion of polyethylene, the overheating of the geomembranes in the sun leads to the formation of wrinkles during installation (Giroud and Peggs, 1990).

These wrinkles may create issues when seaming geomembrane panels and placing protective soil or drainage material on top of the geomembrane (Giroud and Morel, 1992). In addition, they may become snagged or folded when the overlaying material is put in place. They may also obstruct the liquid flow in drainage layers or intensify leakage in composite liners. Geomembranes also age more rapidly at high temperatures (Rowe and Sangam, 2002). This is especially critical at the location of wrinkles, which have been shown to be warmer by as much as 19°C in comparison with locations where the contact between the geomembrane and the soil is good (Take et al. 2014). In the case of slopes, increased desiccation has also been reported in clay subgrades or composite clay liners below the geomembrane, because of the increased evaporation from the subgrade as the geomembrane temperature rises (Basnett and Brungard, 1992).

As a result, geomembranes with a light-reflective surface layer have been developed over the last 25 years (Mathieson and Cadwallader, 1992). The light reflective surface is generally obtained by dispersing titanium dioxide white pigments in the polymer matrix. The effect of the light-reflective surface layer on the geomembrane temperature was studied with smooth white- and white/grey-surfaced HDPE geomembranes and smooth and textured black geomembranes that were placed on a layer of sand and exposed to sunlight (Cadwallader et al. 1993). A 3µm-diameter bead thermocouple was heat-bonded onto the geomembrane surface. With air and sand temperatures at 32°C and 35°C respectively, the difference in temperature between the white-surfaced and the black geomembranes reached 24°C. The smooth white geomembrane was at 43°C on average, the white/gray geomembrane at 49°C, the textured black geomembrane at 64°C, and the smooth black geomembrane at 67°C.

In another experiment involving solar exposure, the temperature of white-surfaced and black HDPE geomembranes, both smooth and textured, was recorded on a clear and sunny day on four occasions over a year, each at a different season, at a site near Philadelphia, PA (Koerner and Koerner, 1995). Thermocouples were attached onto the geomembrane surface using a drop of HDPE extrudate. Temperature differences of 7 to 13°C depending on the season were recorded between the white-surfaced and black geomembrane. On the other hand, no major difference between the smooth and textured samples was observed for both the white-surfaced and the black geomembrane. Another study involved white, light grey, regal blue, and dark grey thermoplastic polyolefin (TPO) roofing membranes exposed to sunlight in the summer of 2009 in Gainesville, TX (Xing and Taylor, 2011). The authors reported that the maximum surface temperature of the membranes was proportional to the product solar reflectance.

Experiments were also conducted using artificial controlled solar conditions (Pelte et al. 1994). An HDPE geomembrane with a coextruded 0.1-mm thick white, glossy coating exhibited a surface temperature of 75°C compared to 110°C for the black only geomembrane. The authors also studied the impact of laying a white nonwoven geotextile on the black geomembrane; it only produced a delay in the heating without reducing the final temperature.

This study aims at complementing the information already available by quantifying the resulting difference in thermal expansion of HDPE geomembranes under solar irradiation associated with the presence of the white surface layer. The irradiance and temperature developed under natural exposure are correlated with the laboratory-controlled artificial conditions. Introducing the thermal expansion of polyethylene geomembranes, a daily expansion is estimated with seasonal climatic fluctuations. The temperature difference between white-surfaced and black geomembranes and its correlation with climatic data are used to quantify the generation of wrinkles caused by specific climate and season conditions.

2 EXPERIMENTAL

2.1 Materials

Two 1.5 mm-thick, smooth HDPE geomembranes were used for the study. They were produced in a 3-layer blown-film coextrusion line. In one of them, all three layers used the same black formulation. For the other one, titanium dioxide powder and hindered amines dispersed in the HDPE matrix was used for the 0.1-mm thick white skin on one side of the geomembrane.

2.2 Artificial UV light exposure testing

Heat generation in the geomembranes was measured under artificial UV light exposure, simulated by Xenon-arc lamps, using the test methodology described in (Dolez et al., 2017).

2.2.1 Specimen preparation

Square specimens of 150 mm side length were prepared from the two types of geomembranes using a configuration allowing probing the geomembrane temperature on the back, unexposed surface. A gauge 30, type-J mini-thermocouple (Omega, Canada) was heat-pressed at the center of the specimen on the surface opposite to light exposure (Figure 1). Dolez et al. (2017) reported a good reproducibility with this configuration; the positioning of the probe was more precise and the contact with polyethylene better than with other configurations tested. A 150 x 150 mm piece of white-surfaced geomembrane was glued on the back of the specimen with the white surface facing towards the outside to prevent any parasitic light absorption from the back of the specimen. Three replicates were prepared.

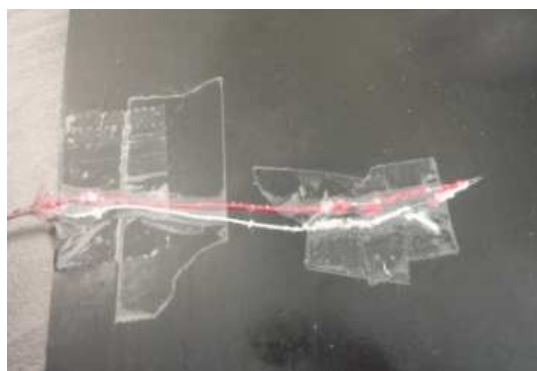


Figure 1. Back of specimen with the hot-pressed thermocouple.



Figure 2. Insulation board closing the Xenon-arc chamber.

2.2.2 Test set-up

The specimens were exposed to solar irradiation using a Xenon-arc chamber operated according to ASTM G155 with a borosilicate filter (Atlas, USA). This system was selected to provide a good match to the daytime solar spectrum. The equipment was modified for the temperature measurements by installing a foam insulation board with an aluminum coating to close the chamber opening (Figure 2).

The specimens were suspended on the sample holding carousel of the Xenon-arc chamber. They were distributed on three rows in the front half of the carousel (Figure 3).

2.2.3 Testing procedure

Three irradiances were selected for the study: 0.17 W/m², 0.35 W/m², and 0.55 W/m². They correspond to daytime irradiances in Toronto, Canada, from March to July. They were controlled at a wavelength of 340 nm. For each of the irradiance values, the temperature of the Xenon-arc chamber was adjusted at 35°C, 45°C, 55°C, and 65°C. The temperature of the black-panel was maintained 30°C lower than the chamber temperature. All trials were conducted with the carousel rotation disabled. For each condition (irradiance and chamber temperature), the temperature measurements were carried out after a 60-min stabilization period.

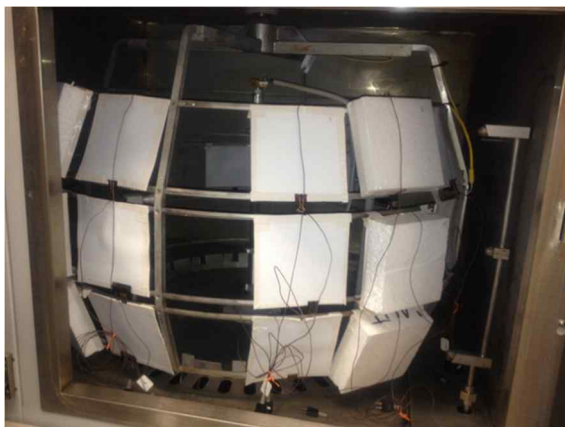


Figure 3. Specimens installed in the carousel of the Xenon-arc chamber.



Figure 4. Specimen setup for CTE measurement, using tension clamps.

2.3 Thermal expansion coefficient measurement

The coefficient of thermal expansion (CTE) was determined by thermomechanical analysis in accordance with ASTM E831 using a dynamic mechanical analyzer operated in transient mode (Beaumier et al., 2017).

The test was carried out by holding the stress applied to the specimen constant and recording the increase in deformation as the temperature is gradually raised. According to the indications of the manufacturer, the high-resolution linear optical encoder used to measure displacements allows reaching a strain resolution of 1 nm. Tension clamps, shown in Figure 4, were used to secure the 6.27 mm wide geomembrane specimens. The initial specimen length was 16.1 mm. The test used a 0.3°C/min heating rate and an applied force set at zero. A 1.68 x 4.53 x 25 mm quartz prism was used to compute the correction to apply for the expansion of the sample holder.

3 RESULTS

3.1 Comparison of geomembrane temperatures

Figure 5 shows the temperature variation for the white-surfaced and black geomembranes as a function of the irradiance at 65°C. Individual data points correspond to the three replicates for each condition. A relatively good reproducibility in the temperature measurements is observed, with variations between replicates less than 10%. An increase in the geomembrane temperature with the irradiance is recorded, for both white-surfaced and black geomembranes. The temperature of the black membrane for a given irradiance is systematically above that of the white-surfaced membrane. A similar behavior was observed at the three other chamber temperatures tested, as shown in Figure 6 for the white-surfaced geomembrane.

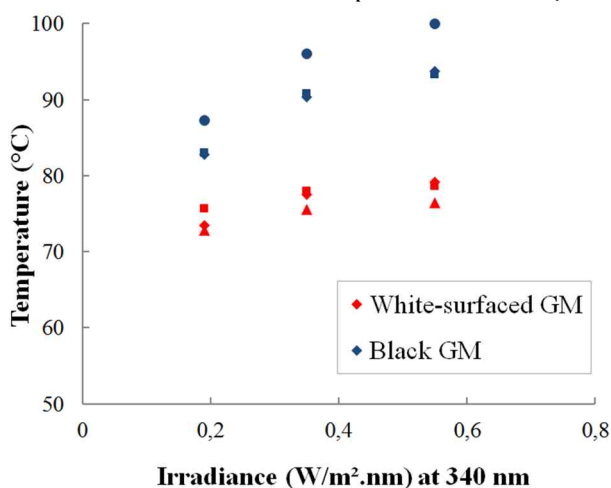


Figure 5. Geomembrane temperature as a function of the irradiance at 65°C. the white-surfaced geomembrane.

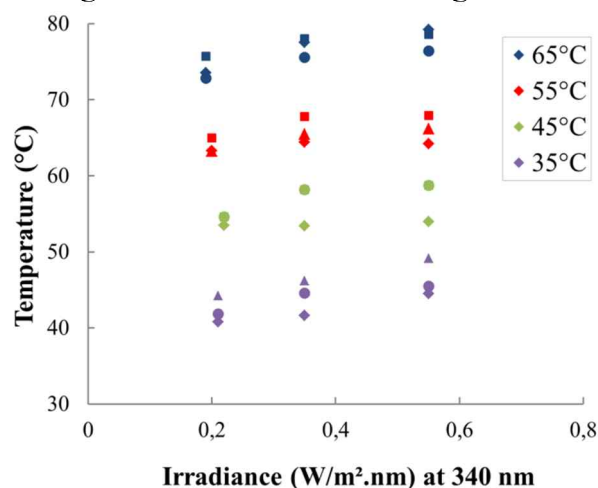


Figure 6. Geomembrane temperature vs. irradiance for the white-surfaced geomembrane.

Figure 7 shows the temperature difference between the chamber air and the white-surfaced geomembrane as a function of irradiance. The variation of the temperature difference ($\Delta T_{WGM-AIR}$) in °C as a function of the irradiance (E_{340nm}) in $W/m^2 \cdot nm$ may be described by a power-law relation:

$$\Delta T_{WGM-AIR} = 14.1(E_{340nm})^{0.324} \quad (1)$$

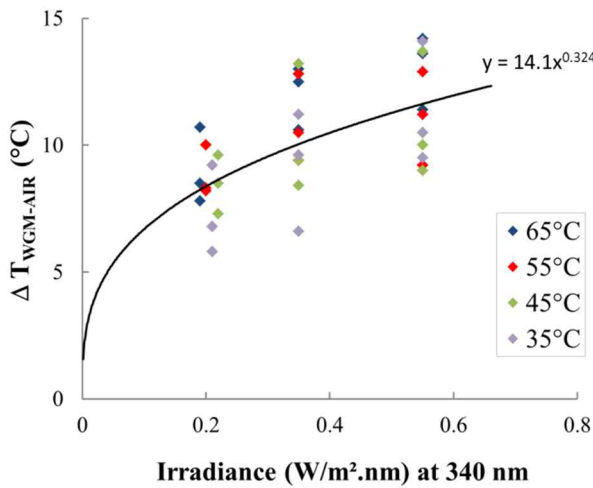


Figure 7. Temperature difference between the white-surfaced geomembrane and the air in the chamber.

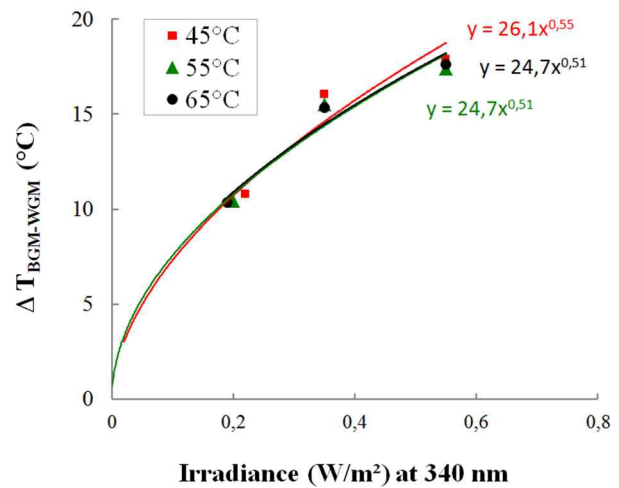


Figure 8. Temperature difference between the black and white-surfaced geomembrane, with data fit by a power-law function.

3.2 Modelling of temperature difference between the white-surfaced and the black geomembranes

The difference in the average temperature between the white-surfaced and the black geomembrane, $\Delta T_{BGM-WGM}$, expressed as a function of the irradiance for the different chamber temperatures tested is shown in Figure 8. No significant effect of the chamber temperature is observed. This result is in agreement with the absence of trend in the data recorded by Koerner and Koerner (1995) in the field over different seasons. A power-law regression was applied to the data. It led to the following relations:

$$\text{For an air temperature of } 45^\circ\text{C:} \quad \Delta T_{BGM-WGM} = 26.1(E_{340nm})^{0.55} \quad (2)$$

$$\text{For an air temperature of } 55^\circ\text{C and above:} \quad \Delta T_{BGM-WGM} = 24.7(E_{340nm})^{0.51} \quad (3)$$

3.3 Coefficient of thermal expansion

Figure 9 shows the variation in the specimen clamp displacement as a function of the temperature for the white-surfaced geomembrane in the machine direction. The CTE values computed by the secant method are shown for three different temperatures between 30 and 50°C.

These CTE values are plotted as a function of temperature in Figure 10. It can be observed that the CTE increases with temperature, even though it is often presented as a constant for polyethylene. It is also higher than what is commonly published for measurements made according to ASTM D696 with a vitreous silica dilatometer (2016). This may be attributed to the fact that, when measured according to ASTM D696, the test specimen is exposed to a relatively high compressive stress, i.e. in the range of 70 kPa. On the other hand, CTE measurements performed here with the thermomechanical analysis involved a very small tensile stress, which may better reflect the actual, field behavior of a geomembrane laid flat on soil.

Based on the fact that CTE has always a positive value for polyethylene, an exponential regression is proposed for projecting CTE values at temperatures lower than 40°C. Field observations have also shown that thermal contraction and expansion taking place at sub-zero temperatures are of a lesser magnitude than those taking place in warm weather, for a similar temperature differential.

The following relation was thus considered for the variation of CTE with temperature in Fig. 10:

$$CTE = 328 e^{(0.0094T)} \quad (4)$$

4 DISCUSSION

In an attempt to quantify the impact of white-surfaced geomembranes in a realistic field scenario, a projection was made using climatic data in Toronto, Canada (Environment Canada, 2006). Irradiance was measured between 295 nm and 325 nm using a pyranometer and expressed in W/m².nm. A proportional relationship with the controlled irradiance of Xenon-arc lamps at 340 nm is assumed using the solar distribution provided in ASTM G173, for direct normal irradiance at the average latitude in the USA (Figure 11). Irradiance at 340 nm thus corresponds to 19.8% of the cumulative irradiance from 295 to 325 nm.

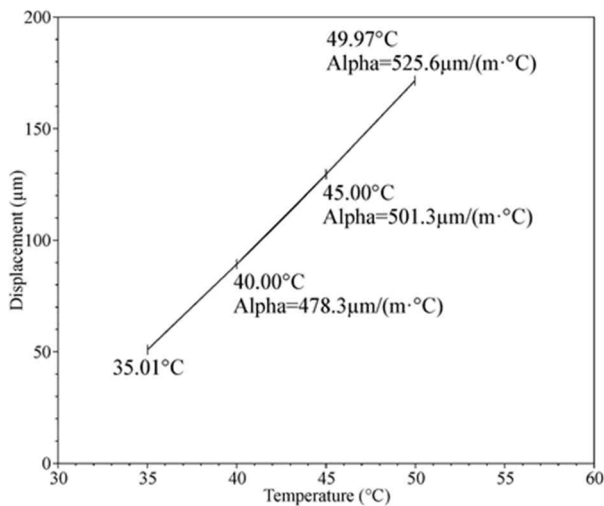


Figure 9. Determination of the CTE for the white-surfaced geomembrane, in the machine direction.

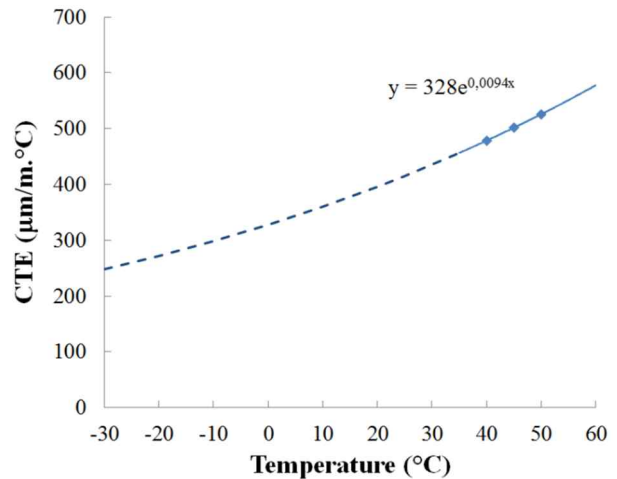


Figure 10. Variation of the white-surfaced geomembrane CTE with temperature, in the machine direction.

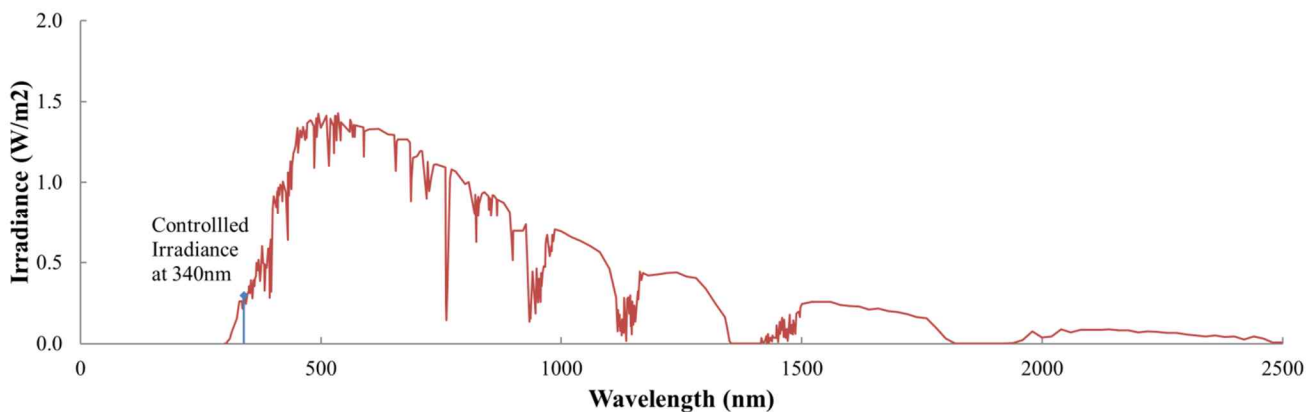


Figure 11. Spectral solar distribution of sunlight as per ASTM G173, and its relative fraction of energy at 340nm, used as controlled irradiance for the exposure to Xenon-Arc lamps in artificial weathering chambers.

However, climate experiences seasonal variations in temperature and irradiance. For instance, Figure 12 shows seasonal temperature and irradiance change recorded in 2011 at the Toronto Pearson Airport, Canada; both follow a similar trend. Daily temperature and irradiance fluctuations (Figure 13) also affect exposed geomembranes and may lead to wrinkles.

Combining Equations (1) to (4) and the seasonal and daily variations in temperature and irradiance (Fig. 12 and 13), the geomembrane daily thermal expansion in Toronto (dL) is calculated as a function of the daily peak irradiance (Fig. 14) and the season (Fig. 15) using the following equation:

$$dL = L \int_{T_{min}}^{T_{max}} \alpha x 328 e^{(0.0094 T)} dT \tag{5}$$

With L, the reference length (100m) and T, the temperature in °C. T_{min} is the minimum daily air temperature and T_{max} is given by the following relations:

For black geomembrane: $T_{max} = T_{daily,max} + \Delta T_{WGM-AIR} + \Delta T_{BGM-WGM}$ (6)

For white-surfaced geomembrane: $T_{max} = T_{daily,max} + \Delta T_{WGM-AIR}$ (7)

Where $T_{daily,max}$ is the maximum daily temperature from the climatic data (air temperature in the shadow).

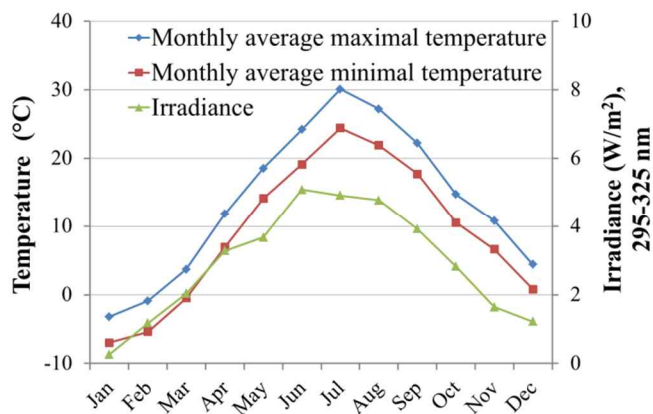


Figure 12. Seasonal fluctuations at Toronto Pearson Airport, Canada, measured in 2011.

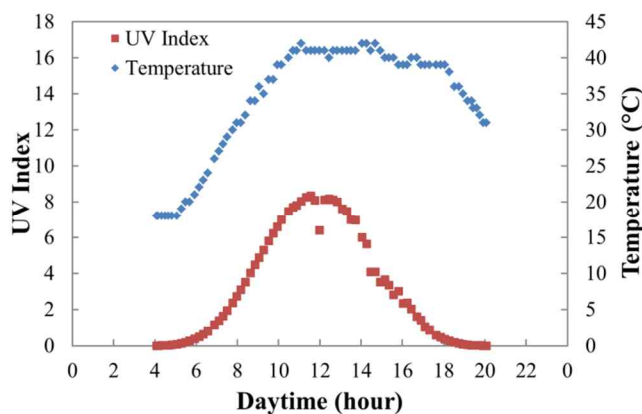


Figure 13. Daily UV index cycle on July 1st, 2011, in Toronto, Canada.

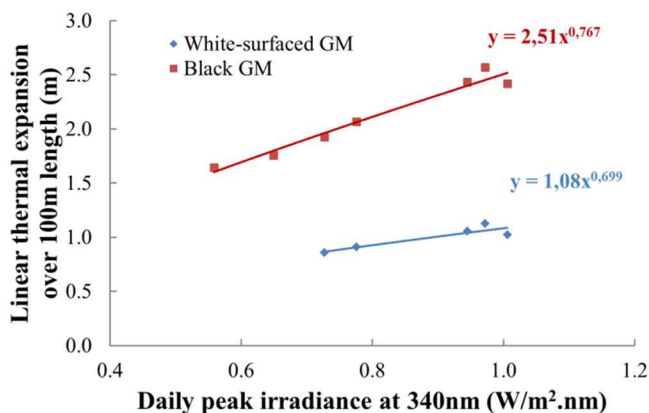


Figure 14. Estimate of linear thermal expansion of geomembranes, in machine direction, for Toronto.

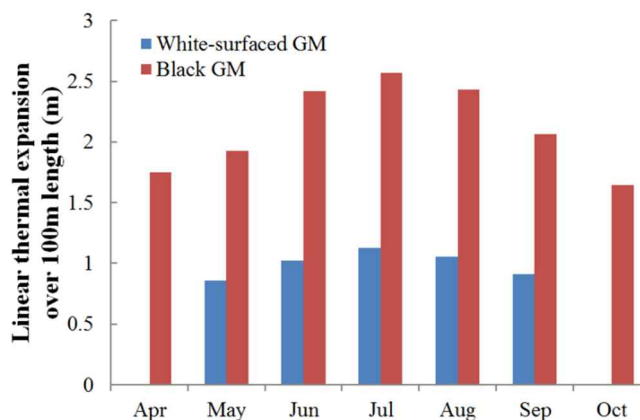


Figure 15. Effect of seasonal fluctuations on the thermal expansion of geomembranes in Toronto.

This analysis shows that white-surfaced geomembranes experience a reduction of 55 to 60% in daily thermal expansion at the maximum yearly sunlight and temperature in Toronto, Canada. Previous studies (Beaumier et al., 2017; Denis, 2015) have estimated to 10 to 20°C the difference between the black and white-surfaced geomembranes, resulting in a 0.15 to 0.3 m reduction in wrinkle width for a 100 m long geomembrane panel. However, these studies underestimated the contribution of white-surfaced geomembranes in reducing thermal expansion because they did not consider the peak irradiance energy of natural sunlight. In addition, thermal expansion was underestimated due to the use of a dilatometer for the measurements. The fact that thermal expansion varies with temperature (Fig. 9 and 10) was also not taken into account. When these different factors are considered, the temperature of the black geomembrane is estimated to be up to 25°C higher than that of the white-surfaced geomembrane under Toronto’s summer sunlight. The difference in width and number of wrinkles is thus much larger if one considers a thermal expansion about 2 to 3 times larger for the black geomembrane than the white-surfaced one.

Other field considerations could also influence the resulting geomembrane temperature. For instance, the number and size of wrinkles affect the contact area between the geomembrane and the underneath material or subgrade. Usually the ground is at a lower temperature than the exposed surface; increased thermal conduction between the white-surfaced geomembrane and its subgrade will contribute to evacuate an even larger amount of heat from solar radiation. Other factors such as wind, slope, ground temperature, and humidity for instance may also play a role.

Based on these results, the use of this analysis could lead to a comprehensive understanding of slack calculation, that can be used for the installation of geomembranes.

5 CONCLUSION

This study has looked at the effect of the presence of a white layer on the surface of black geomembranes on heat generation under solar irradiation. The evaluation combines the measurement of geomembrane temperature under artificial weathering, and the measurement of the coefficient of thermal expansion by thermomechanical analysis. Based on environmental data obtained for Toronto, Canada, a reduction of 55 to 60% in thermal expansion was computed for white-surfaced geomembranes compared to black geomembranes at the maximum yearly sunlight and temperature conditions. The temperature of the black geomembrane is estimated to be up to 25°C higher than the white-surfaced geomembrane under Toronto's summer sunlight. The larger values reported here can be attributed to the fact that previous studies did not consider the peak irradiance energy of natural sunlight, used dilatometer for the determination of CTE, and did not take into account the variation of polyethylene thermal expansion with temperature.

The study also provides additional information for installation purposes. Daily thermal expansion was calculated for different periods of the year and can be used to compute slack correction for instance. Benefits to installation and service life include large improvements in the ease of installation and backfilling, reduced risk of subgrade desiccation and leakage, and reduced geomembrane aging rate among others. White-surfaced geomembranes therefore appear to be an attractive option for exposed applications where large fluctuations in solar radiation are expected over short periods, for example within a day.

ACKNOWLEDGEMENTS

This project benefits from a financial support from the Natural Sciences and Engineering Research Council of Canada (NSERC) through its Applied Research and Development program. The authors also want to thank Mr. Soufiane Fath who contributed to the experimental work.

REFERENCES

- ASTM D696. 2016. *Standard test method for coefficient of linear thermal expansion of plastics between -30°C and 30°C with a vitreous silica dilatometer*. ASTM International.
- ASTM G155-13. 2013. *Standard Practice for Operating Xenon Arc Light Apparatus for Exposure of Non-Metallic Materials*. ASTM International.
- ASTM G173-03. 2012. *Standard Tables for Reference Solar Spectral Irradiances: Direct Normal and Hemispherical on 37° Tilted Surface*. ASTM International.
- Basnett, C. & Brungard, M. 1992. *Geotechnical Fabrics Report*, Vol. 10(1), pp. 38-41.
- Beaumier D., Dolez P. I., Blond E. 2017. *Geotechnical Frontiers 2017*, Vol. GSP 280, pp. 227-235.
- Cadwallader, M., Cranston, M., & Peggs, I. D. 1993. *Geosynthetics '93*, pp. 1065-1079.
- Denis, R. 2015. *25th Annual Solid Waste Technical Conference*.
- Dolez P.I., Beaumier D., Taghizadeh T., Blond E. 2017. *Geotechnical Frontiers 2017*, Vol. GSP 276, pp. 259-266.
- Environment Canada. 2006. *Guide to the WMO/GAW World Ultraviolet Radiation Data Centre*, Version 6.0.
- Giroud, J.P. & Morel N. 1992. *Geotextiles and Geomembranes*, Vol. 11, pp. 255-276.
- Giroud, J.P. & Peggs, I.D. 1990. In: *Waste containment systems: construction, regulation and performance*. ASCE. pp. 190-225.
- Koerner, G.R. & Koerner, R.M. 1995. *Geosynthetics '95*, pp. 921-937.
- Mathieson, M.C. & Cadwallader, M.W. 1992. *Apparatus and method for lining landfills, reservoirs, hazardous waste disposal sites and the like*. US Patent 5,139,853. United States Patent and Trademark Office.
- Pelte, T., Pierson, P., & Gourc, J.P. 1994. *Geosynthetics International*, Vol. 1(1), pp. 21-44.
- Rowe, R.K. 1998. *Proc. 6th International Conference on Geosynthetics*, pp. 27-103.
- Rowe, R.K. & Ewais, A.M.R. 2015. *Canadian Geotechnical Journal*, Vol. 52(3), pp. 326-343.
- Rowe, R.K., Rimal, S., & Sangam, H.P. 2009. *Geotextiles and Geomembranes*, Vol. 27(2), pp. 137-151.
- Rowe, R.K. & Sangam, H.P. 2002. *Geotextiles and Geomembranes*, Vol. 20, pp. 77-95.
- Scheirs, J. 2009. *A Guide to Polymeric Geomembranes*. John Wiley & Sons, Chichester, UK.
- Struick, L.C.E. 1985. *Encyclopedia of Polymer Science and Engineering*, John Wiley & Sons. Vol. 4, pp. 630-696.
- Take, W.A., Brackman, R.W.I., & Rowe, R.K. 2014. *IGS 10*, 8p.
- Xing, L. & Taylor, T.J. 2011. *Journal of ASTM International*, Vol. 8(8), 14p.